9874 *Inorg. Chem.* **2009**, *48*, 9874–9882
DOI: 10.1021/ic901563n

Inorganic Chemistry
Article

Isostructural Bis-1,2,3-Thiaselenazolyl Dimers

Alicea A. Leitch,[†] Xueyang Yu,[‡] Craig M. Robertson,[†] Richard A. Secco,[‡] John S. Tse,[§] and Richard T. Oakley*,[†]

[†]*Department of Chemistry, University of Waterloo, Waterloo, Ontario N2L 3G1, Canada,* [‡]*Department of Earth Sciences, University of Western Ontario, London, Ontario N6A 5B7, Canada, and* [§]*Department of Physics and Engineering Physics, University of Saskatchewan, Saskatoon, Saskatchewan S7N 5E2, Canada*

Received August 5, 2009

Reduction of the *N*-methylated bis-1,2,3-thiaselenazolylium salts [**2a**,**b**,**c**][OTf] (with R_1 = Me and R_2 = H (**2a**), F (**2b**), Me (**2c**)) affords the corresponding bis-1,2,3-thiaselenazolyl radicals **2a**,**b**,**c**. The radicals crystallize as centrosymmetric Se−Se σ-bonded dimers [**2a**,**b**,**c**]$_2$, in which an intramolecular Se−S bond of the radical is cleaved and replaced by an intermolecular Se−Se bond. The crystal structures of the three dimers are isomorphous, all belonging to the monoclinic space group $P2_1/c$, and consist of interpenetrating, cross-braced, slipped π-stack arrays laced together by numerous short intermolecular Se—N′ and Se—S′ contacts. In the solid state the dimers are diamagnetic, and behave as small band gap semiconductors with a room temperature conductivity σ_{RT} near 10^{-6} S cm^{-1}. Application of pressure leads to a dramatic increase in conductivity for all three compounds. At 5 GPa the value of σ_{RT} ranges from near 10^{-1} S cm^{-1} for [**2c**]$_2$ to 1 S cm^{-1} for [**2b**]$_2$ and 10^1 S cm^{-1} for [**2a**]$_2$. Comparison of the three crystal structures suggests that the compressibility of [**2a**]$_2$, and hence the response of its conductivity to pressure, is superior to that of [**2b,c**]$_2$.

Introduction

Molecular solids typically exhibit low electrical conductivity, as charge carriers must be generated by thermal activation across a band gap, the magnitude of which depends on the energy difference between the highest occupied and lowest unoccupied molecular orbitals (the HOMO and LUMO). Even in condensed ring aromatic hydrocarbons this gap is large. The conventional approach to developing conductivity in molecular compounds therefore involves the use of charge transfer (CT) to create charge carriers by depleting a valence band and/or partially filling a conduction band.[1,2] Typically, two components, a donor and an acceptor, are required, although single component metals have been generated by incorporating the two moieties into a single compound and then fine-tuning the HOMO−LUMO gap.[3] In principle, neutral π-radicals represent an appealing alternative to the CT paradigm, as they provide, within the context of a single component system, the necessary electronic features for conductivity.[4] Ideally, a π-stacked array of radicals, each with one unpaired electron, should afford a half-filled energy band, and a metallic ground state. This simple picture is, however, compromised by two shortcomings. The first problem is that radicals tend to associate, affording discrete dimers or insulating charge-density-wave states. The second difficulty is associated with the onsite Coulomb potential U, the barrier to electron transfer, which is a maximum for a half-filled band (an $f = 1/2$ system). Thus, when dimerization can be suppressed, the electronic bandwidth W arising from the overlap of the singly occupied molecular orbitals (SOMOs) of adjacent radicals is insufficient to overcome the large U value, and a Mott insulating state prevails.[5]

*To whom correspondence should be addressed. E-mail: oakley@uwaterloo.ca.

(1) (a) Garito, A. F.; Heeger, A. J. *Acc. Chem. Res.* **1974**, *7*, 232. (b) Torrance, J. B. *Acc. Chem. Res.* **1979**, *12*, 79. (c) Williams, J. M.; Ferraro, J. R.; Thorn, R. J.; Carlson, K. D.; Geiser, U.; Wang, H. H.; Kini, A. M.; Whangbo, M.-H. *Organic Superconductors* (*Including Fullerenes*); Prentice Hall: Englewood Cliffs, 1992.

(2) (a) Bendikov, M.; Wudl, F.; Perepichka, D. F. *Chem. Rev.* **2004**, *104*, 4891. (b) Jérome, D. *Chem. Rev.* **2004**, *104*, 5565. (c) Geiser, U.; Schlueter, J. A. *Chem. Rev.* **2004**, *104*, 5203. (d) Yamada, J.; Akutsu, H.; Nishikawa, H.; Kikuchi, K. *Chem. Rev.* **2004**, *104*, 5057. (e) Saito, G.; Yoshida, Y. *Bull. Chem. Soc. Jpn.* **2007**, *80*, 1.

(3) (a) Tanaka, H.; Okano, Y.; Kobayashi, H.; Suzuki, W.; Kobayashi, A. *Science* **2001**, *291*, 285. (b) Tanaka, H.; Tokumoto, M.; Ishibashi, S.; Graf, D.; Choi, E. S.; Brooks, J. S.; Yasuzuka, S.; Okano, Y.; Kobayashi, H.; Kobayashi, A. *J. Am. Chem. Soc.* **2004**, *126*, 10518. (c) Kobayashi, A.; Sasa, M.; Suzuki, W.; Fujiwara, E.; Tanaka, H.; Tokumoto, M.; Okano, Y.; Fujiwara, H.; Kobayashi, H. *J. Am. Chem. Soc.* **2004**, *126*, 426. (d) Kobayashi, A.; Fujiwara, E.; Kobayashi, H. *Chem. Rev.* **2004**, *104*, 5243.

(4) (a) Haddon, R. C. *Nature* **1975**, *256*, 394. (b) Haddon, R. C. *Aust. J. Chem.* **1975**, *28*, 2333. (c) Haddon, R. C. *Aust. J. Chem.* **1975**, *28*, 2343.

(5) (a) Mott, N. F. *Metal-insulator Transitions*; Taylor and Francis: London, 1990.(b) Whangbo, M.-H. *J. Chem. Phys.* **1979**, *70*, 4963. (c) Friedel, J.; Noguera, C. *Int. J. Quantum Chem.* **1983**, *23*, 1209. (d) Huang, J.; Kertesz, M. *J. Phys. Chem. A* **2007**, *111*, 6304.

(6) (a) Goto, K.; Kubo, T.; Yamamoto, K.; Nakasuji, K.; Sato, K.; Shiomi, D.; Takui, T.; Kubota, M.; Kobayashi, T.; Yakusi, K.; Ouyang, J. *J. Am. Chem. Soc.* **1999**, *121*, 1619. (b) Koutentis, P. A.; Chen, Y.; Cao, Y.; Best, T. P.; Itkis, M. E.; Beer, L.; Oakley, R. T.; Brock, C. P.; Haddon, R. C. *J. Am. Chem. Soc.* **2001**, *123*, 3864. (c) Takano, Y.; Taniguchi, T.; Isobe, H.; Kubo, T.; Morita, Y.; Yamamoto, K.; Nakasuji, K.; Takui, T.; Yamaguchi, K. *J. Am. Chem. Soc.* **2002**, *124*, 11122. (d) Beer, L.; Mandal, S. K.; Reed, R. W.; Oakley, R. T.; Tham, F. S.; Donnadieu, B.; Haddon, R. C. *Cryst. Growth Des.* **2007**, *7*, 101.

Published on Web 09/18/2009
© 2009 American Chemical Society

Chart 1

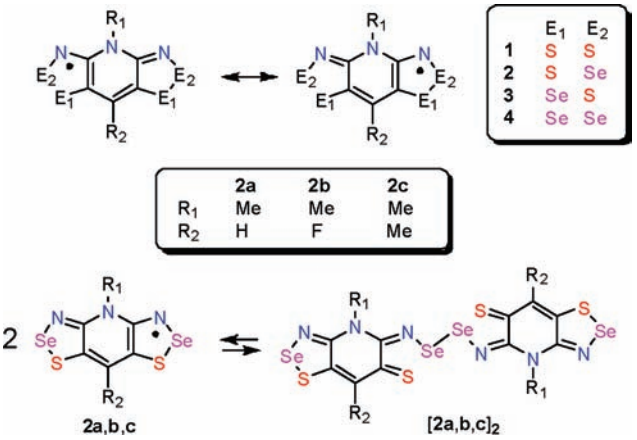

Considerable progress has been made toward overcoming both of these design challenges, and a number of organic radicals exhibiting high (albeit not metallic) conductivity have been generated.[6,7]

In recent years we have explored the synthesis and characterization of heavy atom heterocyclic radicals based on the bisdithiazolyl framework **1** (Chart 1). These highly delocalized radicals display low gas phase disproportionation energies ΔH_{disp} and solution-based cell potentials E_{cell},[8] features which augur well for low values of the onsite Coulomb potential U.[9] However, their slipped π-stack structures compromise intermolecular overlap and hence bandwidth W, as a result of which their room temperature conductivities σ_{RT} are generally low, near 10^{-6} S cm^{-1}.[10] Improvements in conductivity have been made by designing superimposed π-stack structures,[11] or by the incorporation of the heavier, more spatially extensive heteroatom selenium, as in **2**, **3**, and **4**.[12] In addition to possessing improved charge transport properties,[13] some of these selenium-based radicals have shown interesting magnetic behavior. Radicals **3** and **4** (R_1 = Et, R_2 = H), for example, undergo phase transitions to spin-canted antiferromagnetic states with ordering temperatures of 18 and 27 K, respectively,[14] while **2** and **4** (R_1 = Et, R_2 = Cl) order as bulk ferromagnets with T_c values of 12.8 and 17.0 K.[15,16] The latter are among the highest ordering temperatures ever observed for non-metal based ferromagnetic materials.

For a given combination of exocyclic ligands R_1 and R_2, most (but not all)[13] radicals **1**−**4** form isostructural sets in the solid state. In one early case, namely, **2** (R_1 = Me, R_2 = H, hereafter referred to as **2a**), the radical crystallized as centrosymmetric σ-bridged dimer $[\mathbf{2a}]_2$.[17] Although dimerization of selenium centered radicals is well-known,[18,19] this lateral mode of association was, at the time, without precedent. Variable temperature magnetic susceptibility and conductivity measurements established that $[\mathbf{2a}]_2$ is a diamagnetic small band gap semiconductor with a room temperature conductivity σ(298 K) near 10^{-6} S cm^{-1} and thermal activation energy E_{act} of 0.32 eV. While these values were, by themselves, notable, what made this material remarkable was the dependence of its conductivity and activation energy on pressure. Under an applied pressure of 5 GPa the conductivity of $[\mathbf{2a}]_2$ was increased by 5 orders of magnitude, and E_{act} dropped to near 0.03 eV. For closed shell molecular compounds such responses are extremely rare, and typically require much higher pressures.[20] For example, the activation energy E_{act} of single crystals of pentacene can be reduced to zero near 27 GPa,[21] although for powdered samples higher pressures are required. Selenium[22] and tellurium-substituted

(7) (a) Chi, X.; Itkis, M. E.; Patrick, B. O.; Barclay, T. M.; Reed, R. W.; Oakley, R. T.; Cordes, A. W.; Haddon, R. C. *J. Am. Chem. Soc.* **1999**, *121*, 10395. (b) Pal, S. K.; Itkis, M. E.; Tham, F. S.; Reed, R. W.; Oakley, R. T.; Haddon, R. C. *Science* **2005**, *309*, 281. (c) Mandal, S. K.; Samanta, S.; Itkis, M. E.; Jensen, D. W.; Reed, R. W.; Oakley, R. W.; Tham, F. S.; Donnadieu, B.; Haddon, R. C. *J. Am. Chem. Soc.* **2006**, *128*, 1982. (d) Pal, S. K.; Itkis, M. E.; Tham, F. S.; Reed, R. W.; Oakley, R. T.; Haddon, R. C. *J. Am. Chem. Soc.* **2008**, *130*, 3942. (e) Haddon, R. C.; Sarkar, A.; Pal, S. K.; Chi, X.; Itkis, M. E.; Tham, F. S. *J. Am. Chem. Soc.* **2008**, *130*, 13683.

(8) ΔH_{disp} is the enthalpy change for the conversion of two gas phase radicals R into a cation/anion pair, i.e., 2 R⇄ R$^+$ + R$^-$, and is equal to the difference between the ionization potential (IP) and electron affinity (EA). The cell potential $E_{cell} = E_{1/2}(ox) - E_{1/2}(red)$ is the difference between the half-wave potentials for the oxidation and reduction processes.

(9) (a) Beer, L.; Brusso, J. L.; Cordes, A. W.; Haddon, R. C.; Itkis, M. E.; Kirschbaum, K.; MacGregor, D. S.; Oakley, R. T.; Pinkerton, A. A.; Reed, R. W. *J. Am. Chem. Soc.* **2002**, *124*, 9498. (b) Cordes, A. W.; Haddon, R. C.; Oakley, R. T. *Phosphorus, Sulfur, Silicon Rel. Elem.* **2004**, *179*, 673.

(10) (a) Beer, L.; Brusso, J. L.; Cordes, A. W.; Haddon, R. C.; Godde, E.; Itkis, M. E.; Oakley, R. T.; Reed, R. W. *Chem. Commun.* **2002**, 2562. (b) Beer, L.; Britten, J. F.; Brusso, J. L.; Cordes, A. W.; Haddon, R. C.; Itkis, M. E.; MacGregor, D. S.; Oakley, R. T.; Reed, R. W.; Robertson, C. M. *J. Am. Chem. Soc.* **2003**, *125*, 14394. (c) Beer, L.; Britten, J. F.; Clements, O. P.; Haddon, R. C.; Itkis, M. E.; Matkovich, K. M.; Oakley, R. T.; Reed, R. W. *Chem. Mater.* **2004**, *16*, 1564.

(11) Leitch, A. A.; Reed, R. W.; Robertson, C. M.; Britten, J. F.; Yu, X.; Secco, R. A.; Oakley, R. T. *J. Am. Chem. Soc.* **2007**, *129*, 7903.

(12) (a) Beer, L.; Brusso, J. L.; Haddon, R. C.; Itkis, M. E.; Oakley, R. T.; Reed, R. W.; Richardson, J. F.; Secco, R. A.; Yu, X. *Chem. Commun.* **2005**, 5745. (b) Brusso, J. L.; Cvrkalj, K.; Leitch, A. A.; Oakley, R. T.; Reed, R. W.; Robertson, C. M. *J. Am. Chem. Soc.* **2006**, *128*, 15080. (c) Brusso, J. L.; Derakhshan, S.; Itkis, M. E.; Kleinke, H.; Haddon, R. C.; Oakley, R. T.; Reed, R. W.; Richardson, J. F.; Robertson, C. M.; Thompson, L. K. *Inorg. Chem.* **2006**, *45*, 10958.

(13) Leitch, A. A.; Yu, X.; Winter, S. M.; Secco, R. A.; Dube, P. A.; Oakley, R. T. *J. Am. Chem. Soc.* **2009**, *131*, 7112.

(14) Leitch, A. A.; Brusso, J. L.; Cvrkalj, K.; Reed, R. W.; Robertson, C. M.; Dube, P. A.; Oakley, R. T. *Chem. Commun.* **2007**, 3368.

(15) (a) Robertson, C. M.; Myles, D. J. T.; Leitch, A. A.; Reed, R. W.; Dooley, D. M.; Frank, N. L.; Dube, P. A.; Thompson, L. K.; Oakley, R. T. *J. Am. Chem. Soc.* **2007**, *129*, 12688. (b) Robertson, C. M.; Leitch, A. A.; Cvrkalj, K.; Reed, R. W.; Myles, D. J. T.; Dube, P. A.; Oakley, R. T. *J. Am. Chem. Soc.* **2008**, *130*, 8414.

(16) Robertson, C. M.; Leitch, A. A.; Cvrkalj, K.; Myles, D. J. T.; Reed, R. W.; Dube, P. A.; Oakley, R. T. *J. Am. Chem. Soc.* **2008**, *130*, 14791.

(17) (a) Beer, L.; Brusso, J. L.; Haddon, R. C.; Itkis, M. E.; Leitch, A. A.; Oakley, R. T.; Reed, R. W.; Richardson, J. F. *Chem. Commun.* **2005**, 1543. (b) Beer, L.; Brusso, J. L.; Haddon, R. C.; Itkis, M. E.; Kleinke, H.; Leitch, A. A.; Oakley, R. T.; Reed, R. W.; Richardson, J. F.; Secco, R. A.; Yu, X. *J. Am. Chem. Soc.* **2005**, *127*, 18159.

(18) (a) Cordes, A. W.; Haddon, R. C.; Oakley, R. T.; Schneemeyer, L. F.; Waszczak, J. V.; Young, K. M.; Zimmerman, N. M. *J. Am. Chem. Soc.* **1991**, *113*, 582. (b) Andrews, M. P.; et al. *J. Am. Chem. Soc.* **1991**, *113*, 3559. (c) Cordes, A. W.; Haddon, R. C.; Hicks, R. G.; Oakley, R. T.; Palstra, T. T. M.; Schneemeyer, L. F.; Waszczak, J. V. *J. Am. Chem. Soc.* **1992**, *114*, 1729. (d) Britten, J. F.; Clements, O. P.; Cordes, A. W.; Haddon, R. C.; Oakley, R. T.; Richardson, J. F. *Inorg. Chem.* **2001**, *40*, 6820. (e) Beer, L.; Cordes, A. W.; Myles, D. J. T.; Oakley, R. T.; Taylor, N. J. *CrystEngComm* **2000**, *2*, 109. (f) Oakley, R. T.; Reed, R. W.; Cordes, A. W.; Craig, S. L.; Graham, S. B. *J. Am. Chem. Soc.* **1987**, *109*, 7745. (g) Bryan, C. D.; Cordes, A. W.; Oakley, R. T.; Spence, R.E.v.H. *Acta Crystallogr. C* **1995**, *51*, 2402. (h) Cordes, A. W.; Glarum, S. H.; Haddon, R. C.; Hallford, R.; Hicks, R. G.; Kennepohl, D. K.; Oakley, R. T.; Palstra, T. T. M.; Scott, S. R. *J. Chem. Soc., Chem. Commun.* **1992**, 1265.

(19) (a) Feeder, N.; Less, R. J.; Rawson, J. M.; Oliete, P.; Palacio, F. *Chem. Commun.* **2000**, 2449. (b) Parvez, M.; Boeré, R. T. *Acta Crystallogr. C* **1995**, *51*, 2118.

(20) Samara, G. A.; Drickamer, H. G. *J. Chem. Phys.* **1962**, *37*, 474.

(21) Aust, R. B.; Bentley, W. H.; Drickamer, H. G. *J. Chem. Phys.* **1964**, *41*, 1856.

(22) (a) Shirotani, I.; Kamura, Y.; Inokuchi, H.; Hirooka, T. *Chem. Phys. Lett.* **1976**, *40*, 257. (b) Onodera, A.; Shirotani, I.; Inokuchi, H.; Kawai, N. *Chem. Phys. Lett.* **1974**, *25*, 296.

Scheme 1

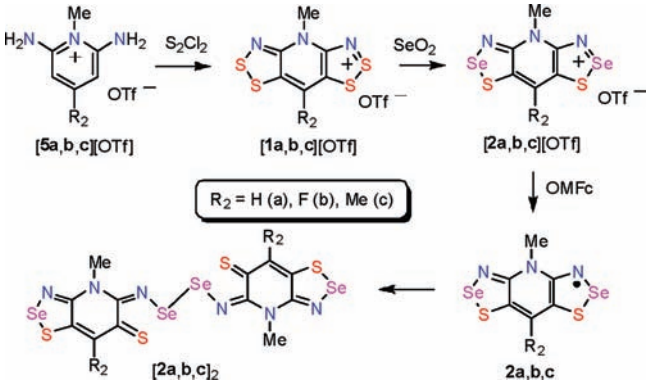

tetracenes have also been shown to display enhanced conductivity under pressure, but metal-like behavior again requires a pressure near 25 GPa.[23]

The question therefore arose as to the cause of this dramatic response, that is, the near metallization of $[\mathbf{2a}]_2$ under relatively mild pressure conditions. Was it a result of decomposition and/or rearrangement, or an intrinsic feature of the packing pattern? With respect to the first possibility, post-pressurization infrared analysis showed no indication of decomposition and, in any case, neither sulfur nor selenium, the two most likely decomposition products, display appreciable conductivities under these pressure conditions.[24,25] To explore the second possibility, that the enhancement in conductivity was a consequence of the solid state structure of the dimer, we have prepared two new σ-bonded dimers $[\mathbf{2b}]_2$ (R = F) and $[\mathbf{2c}]_2$ (R = Me). Structural characterization reveals a similar packing arrangement for the two new materials and, satisfyingly, high pressure conductivity measurements indicate a pressure response comparable to that observed for $[\mathbf{2a}]_2$.

Results

Synthesis. The synthetic sequence to the radical dimers $[\mathbf{2a},\mathbf{b},\mathbf{c}]_2$ is illustrated in Scheme 1. In all three cases the key precursor is the triflate salt of the corresponding *N*-methylated diaminopyridinium cation $[\mathbf{5a},\mathbf{b},\mathbf{c}]^+$. These salts undergo a double Herz cyclization with S_2Cl_2 to afford the triflate salts of the bisdithiazolylium framework $[\mathbf{1a},\mathbf{b},\mathbf{c}]^+$. Conditions for this condensation, and the preparation of the necessary starting pyridinium salt have already been reported for $[\mathbf{2a},\mathbf{c}]^+$.[10b,c] In the case of $[\mathbf{2b}]^+$ the starting material [**5b**][OTf] was prepared by the methylation of 2,4,6-trifluoropyridine and ammination of the subsequent *N*-methylpyridinium salt. The incorporation of selenium, to afford the desired S_2Se_2 cations [**2a**,**b**,**c**][OTf], was accomplished by heating solutions of [**1a**,**b**,**c**][OTf] with selenium dioxide in HOAc or MeCN, a method developed some years ago for the introduction of selenium into the 2-position of simple 1,2,3-dithiazolylium salts.[26] The progress of the reaction was monitored by Electrospray Ionization (ESI) mass spectrometry, which was also used to confirm the absence of S_3Se_1 and S_1Se_3 materials in the resulting products. Finally, reduction of [**2a**,**b**,**c**][OTf] with octamethylferrocene (OMFc) afforded the radicals **2a**,**b**,**c**, which crystallized from solution as the respective dimers $[\mathbf{2a},\mathbf{b},\mathbf{c}]_2$.

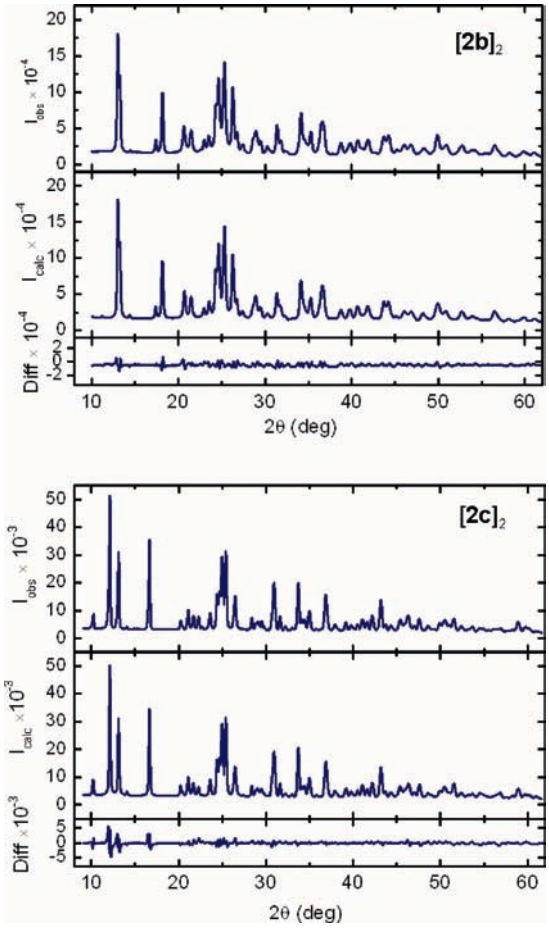

Figure 1. Observed and calculated powder X-ray diffraction patterns for $[\mathbf{2b},\mathbf{c}]_2$ (λ = 1.5406 Å).

Crystal Structures. Crystals of $[\mathbf{2a}]_2$ of sufficient size and quality for single crystal work were obtained by codiffusion of solutions of [**2a**][OTf] and OMFc in acetonitrile.[17] Attempts to extend this approach to $[\mathbf{2b},\mathbf{c}]_2$ were, however, unsuccessful. While these materials could be obtained in good yield and in very pure form, both with respect to chemical and phase composition, neither the size nor the quality of the crystals was suitable for single crystal diffraction. We therefore turned to the use of powder diffraction methods, an approach we have used successfully for the analysis of several related structures.[12b,c] The powder patterns of both $[\mathbf{2b}]_2$ and $[\mathbf{2c}]_2$ were readily indexed using TAUP in terms of the monoclinic space group $P2_1/c$,[27] with cell parameters reminiscent of those found previously for $[\mathbf{2a}]_2$. The structures were solved with simulated annealing methods (DASH and FOX)

(23) Cui, H.; Okano, Y.; Zhou, B.; Kobayashi, A.; Kobayashi, H. *J. Am. Chem. Soc.* **2008**, *130*, 3738.

(24) Selenium enters a metallic phase near 25 GPa.(a) Riggleman, B. M.; Drickamer, H. G. *J. Chem. Phys.* **1962**, *37*, c. (b) Bundy, F. P.; Dunn, K. J. *J. Chem. Phys.* **1979**, *71*, 1550.

(25) Sulfur is converted into a metallic state at pressures above 40 GPa. (a) Chhabildas, L. C.; Ruoff, A. L. *J. Chem. Phys.* **1977**, *66*, 983. (b) Dunn, K. J.; Bundy, F. P. *J. Chem. Phys.* **1977**, *67*, 5048. (c) Peanasky, M. J.; Jurgensen, C. W.; Drickamer, H. G. *J. Chem. Phys.* **1984**, *81*, 6407.

(26) Akulin, Y. I.; Gel'mont, M. M.; Strelets, B. K.; Éfros, L. S. *Khim. Geterotsikl. Soedin.* **1978**, 912.

(27) The $P2_1/c$ space group setting was used (rather than the alternate $P2_1/n$) for $[\mathbf{2b},\mathbf{c}]_2$ to allow for a direct comparison of the two new structures with that of $[\mathbf{2a}]_2$, which had been solved (reference 17) in $P2_1/c$.

Table 1. Crystal Data for $[\mathbf{2a},\mathbf{b},\mathbf{c}]_2$

	$[\mathbf{2a}]_2$ (R_2 = H)[a]	$[\mathbf{2b}]_2$ (R_2 = F)	$[\mathbf{2c}]_2$ (R_2 = Me)
formula	$C_{12}H_8N_6S_4Se_4$	$C_{12}H_6F_2N_6S_4Se_4$	$C_{14}H_{12}N_6S_4Se_4$
fw	680.32	716.30	708.38
a, Å	4.924(4)	4.3792(8)	4.2797(5)
b, Å	12.616(11)	13.3357(31)	13.4739(17)
c, Å	15.086(13)	16.081(4)	17.6545(17)
β, deg	94.563(14)	101.854(22)	100.772(16)
V, Å^3	934.1(14)	919.1(4)	1000.1(2)
ρ(calcd), g cm^{-1}	2.419	2.589	2.352
space group	$P2_1/c$	$P2_1/c$	$P2_1/c$
Z	2	2	2
temp (K)	295(2)	293(2)	293(2)
λ, Å	0.71073	1.54056	1.54056
data/restraints/parameters	2027/0/119		
solution method	direct methods	powder data	powder data
R, R_w (on F^2)	0.0439, 0.0939	0.0493, 0.0585[b]	0.0601, 0.0886[b]

[a] Data from reference 17. [b] R_p and R_{wp} respectively from Rietveld refinements.

Table 2. Selected Distances[a] and Angles[b] in $[\mathbf{2a},\mathbf{b},\mathbf{c}]_2$[c]

	$[\mathbf{2a}]_2$ (R_2 = H)[d]	$[\mathbf{2b}]_2$ (R_2 = F)	$[\mathbf{2c}]_2$ (R_2 = Me)
Se2−Se2′	2.460(2)	2.565	2.530
Se2---S2	2.785(3)	2.790	2.782
S2−C4	1.694(6)	1.694	1.690
Se2−N3	1.816(5)	1.817	1.812
N3−C3	1.298(7)	1.300	1.298
d1, Se2---S1′	3.663(3)	3.651	4.337
d2, S2---S1′	3.616(3)	3.362	3.549
d3, S2---Se1′	3.177(2)	3.086	3.618
d4, S2---S1′	3.268(3)	3.246	3.289
d5, N1---Se1′	2.892(5)	2.963	2.983
δ[e]	3.535(2)	3.509	3.546
τ[f]	45.89(5)	53.24	55.94
θ[g]	174.4(5)	172.8	179.5

[a] Distances in Å. [b] Angles in degrees. [c] For atom numbering, see Chart 2. [d] Data from reference 17. [e] *δ* is the interplanar separation between molecules. [f] *τ* is the tilt angle between the mean molecular plane and the *x* axis. [g] *θ* is the C3−N3−Se2−Se2′ torsion angle within a dimer.

using the known molecular structure of $[\mathbf{2a}]_2$ as an initial model (the basal R_2 = F, Me groups of $[\mathbf{2b},\mathbf{c}]_2$ were introduced in calculated positions). The solutions were then taken into GSAS for final Rietveld refinement. The experimental and final calculated powder patterns are shown in Figure 1; crystal data are provided in Table 1 and a summary of intra- and intermolecular distances and angles is listed in Table 2. An atom numbering scheme is provided in Chart 2.

The crystal structures of $[\mathbf{2a},\mathbf{b},\mathbf{c}]_2$ consist of interpenetrating, cross-braced slipped *π*-stacks of dimers. At the molecular level the three dimers comprise radicals fused at one end by a covalent Se2−Se2′ *σ*-bond. The associated Se2−S2 bond opens to a value intermediate between the sum of the covalent radii[28] and the expected van der Waals contact.[29] Within this supermolecule there is a series of bond length changes relative to those seen in the corresponding cation, the most notable being a shortening of the C3−N3 and C4−S2 distances, all of which

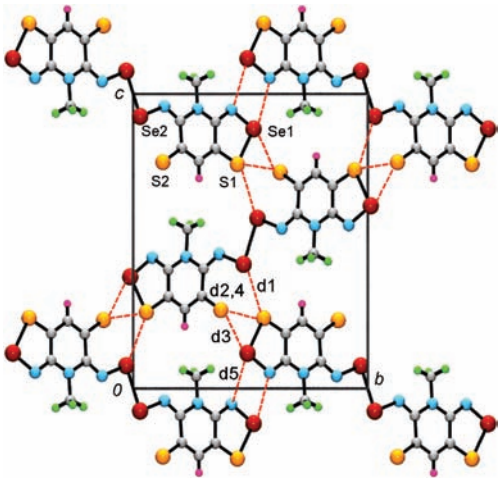

Figure 2. Unit cell of $[\mathbf{2b}]_2$, with intermolecular contacts d1-d5.

Chart 2

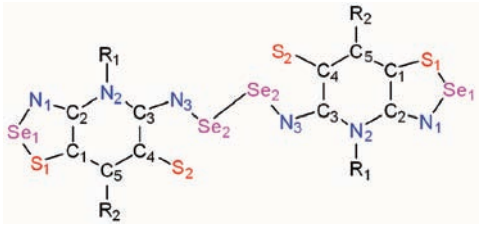

are consistent with the closed shell valence bond formulation $[\mathbf{2}]_2$. Whether the terminal C=S linkages are best referred to as full double bonds is not clear, as aromatic thiones (unless complexed to a metal) are themselves rare.[30] Nonetheless, the C4−S2 distances in $[\mathbf{2a},\mathbf{b},\mathbf{c}]_2$ are comparable to those found in thioureas.[31]

The unit cell drawing of $[\mathbf{2b}]_2$ shown in Figure 2 is representative of the group. This arrangement affords a web of close interdimer S---S′ and S---Se′ interactions d1 to d4. The dimers are also linked laterally into ribbons by four-center Se---N′ contacts d5; these interactions are ubiquitous features in the structures of selenium−nitrogen heterocycles.[32] Neighboring stacks along the *c* axis are tilted in opposite directions so as to give the cross-braced arrangement shown in Figure 3. This side-on view of the slipped *π*-stacks illustrates subtle differences between the three structures. The tilt angle between neighboring dimers along the *c* direction varies with compound, as does the degree of plate slippage along the *π*-stacks. These two structural features are a function of the slippage angle *τ*, which we define as the angle of inclination between the mean molecular plane of the dimer and the stacking axis (the angle at which neighboring dimers along *c* intersect is 2*τ*). The value of *τ*, along

(28) Chen, C. M.; Dojahn, J. G.; Wentworth, W. E. *J. Phys. Chem. A* **1997**, *101*, 3088.
(29) (a) Bondi, A. *J. Phys. Chem.* **1964**, *68*, 441. (b) Dance, I. *New J. Chem.* **2003**, *27*, 22.
(30) Moussa, J.; Lev, D. A.; Boubekeur, K.; Rager, M. N.; Amouri, H. *Angew. Chem., Int. Ed.* **2006**, *45*, 3854.
(31) Venkatachalam, T. K.; Sudbeck, E.; Uckun, F. M. *J. Mol. Struct.* **2005**, *751*, 41.
(32) (a) Cozzolino, A. F.; Vargas-Baca, I.; Mansour, S.; Mahmoudkhani, A. H. *J. Am. Chem. Soc.* **2005**, *127*, 3184. (b) Oakley, R. T.; Reed, R. W.; Robertson, C. M.; Richardson, J. F. *Inorg. Chem.* **2005**, *44*, 1837. (c) Risto, M.; Assoud, A.; Winter, S. M.; Oilunkaniemi, R.; Laitinen, R. S.; Oakley, R. T. *Inorg. Chem.* **2008**, *47*, 10100. (d) Dutton, J. L.; Tindale, J. J.; Jennings, M. C.; Ragogna, P. J. *Chem. Commun.* **2006**, 2474. (e) Berionni, G.; Pégot, B.; Marrot, J.; Goumont, R. *CrystEngComm* **2009**, *11*, 986.

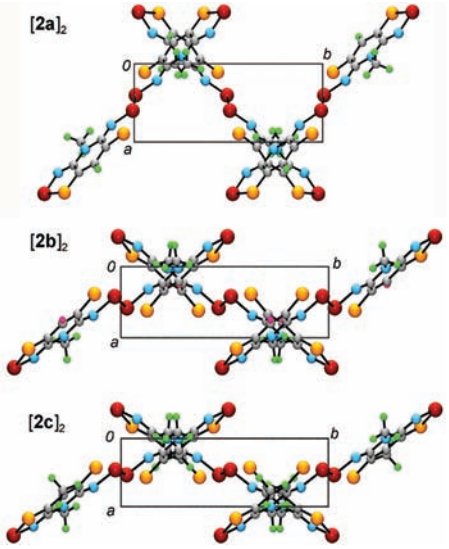

Figure 3. Comparative views of slipped π-stacks in [**2a**,**b**,**c**]$_2$, showing cross-braced architecture.

with the dimer-to-dimer separation along the π-stacks δ, is listed in Table 2. Although δ is fairly consistent across the series (at about 3.5 Å), τ varies over a range of 10°. The degree of plate slippage (τ) is noticeably smaller for [**2a**]$_2$, and accordingly this structure has the steepest tilt angle (2τ) between dimers, as demonstrated in Figure 3. This orientation results in slightly different unit cell dimensions with respect to the other two variants. The remaining two compounds [**2b,c**]$_2$ are more closely related, with similar τ angles and hence packing arrangements. The methyl derivative [**2c**]$_2$, however, has the most severely slipped π-stacks, affording the widest tilt angle between neighboring dimers within the series.

The differences noted above in the degree of slippage of the π-stacks of [**2a,b,c**]$_2$ are associated with changes in the coordination geometry around the diselenide units of the dimers. To illustrate these differences, we show in Figure 4 the respective diselenide "cores", along with the close intermolecular contacts d1−d4. As may be seen from this figure and the metric values in Table 2, all the contacts d1−d4 for [**2a**,**b**]$_2$ are similar in magnitude, but in [**2c**]$_2$ d1 and d3 are considerably larger. Also highlighted in Figure 4 are the intermolecular Me---R$_2$′ contacts. Of these, the Me---CH′ distance in [**2a**]$_2$ is close to the expected van der Waals separation, while the Me---F′ and Me---Me′ contacts in [**2b**,**c**]$_2$ are significantly shorter than the respective van der Waals separations.[29] These more congested interactions may inhibit the compression of the crystal structures of [**2b**,**c**]$_2$ (see below).

Magnetic Measurements

The structural features described above for [**2a**,**b**,**c**]$_2$ are consistent with a closed shell formulation, as depicted in Chart 1. As noted earlier, variable temperature magnetic measurements on [**2a**]$_2$ had indicated essentially diamagnetic behavior, with a small temperature independent paramagnetic component which we ascribed to radical defects. The availability of the two new dimers [**2b**,**c**]$_2$ has provided the opportunity to re-examine more closely the magnetic properties of all three systems, with a view to identifying any

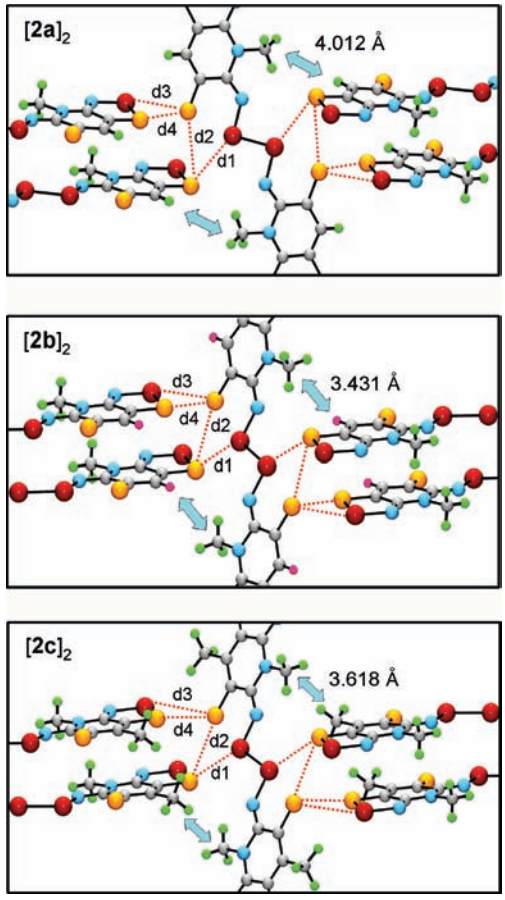

Figure 4. Coordination geometry around the diselenide core of [**2a**,**b**,**c**]$_2$.

structure dependent differences. To that end we have measured the magnetic susceptibility (χ) of [**2a**,**b**,**c**]$_2$ over the temperature range 2−300 K. The results are presented in Figure 5 in the form of plots of χ and χT versus temperature. As may be seen, compounds [**2b**,**c**]$_2$ are, like [**2a**]$_2$, diamagnetic over the entire temperature range, with a weak paramagnetic "tail" appearing in the χ versus T plots at low temperature. This weak paramagnetism is also manifest in the value of χT, which rises to 0.01−0.02 emu K mol^{-1} at 300 K, which can be converted (assuming $g = 2$) to free Curie spin counts (radical defect concentrations) of 2−5%. These concentrations are comparable to those seen in other selenazyl radical dimers.[18]

Conductivity Measurements

To explore the effect of the structural differences noted above on the transport properties of the three dimers [**2a**,**b**,**c**]$_2$ we carried out a series of variable pressure conductivity (σ) measurements using a cubic anvil press. On the basis of our earlier analysis of [**2a**]$_2$, these dimers can be considered as small band gap semiconductors at ambient pressure. In the case of [**2a**]$_2$ the band gap E_g was assessed, by optical and conductivity measurements, to be on the order of 0.5 eV.[17] The results of pressed pellet conductivity measurements on [**2a,b,c**]$_2$ as a function of pressure are shown in Figure 6. As may be seen, all three dimers have similar conductivities σ(298 K) at ambient pressure, that is, values near 10^{-6} S cm^{-1}. Moreover, as in the case for [**2a**]$_2$, the conductivity of both [**2b**,**c**]$_2$ show a strong pressure dependence, with σ(298 K) increasing by 5 to 6 orders of magnitude over the pressure

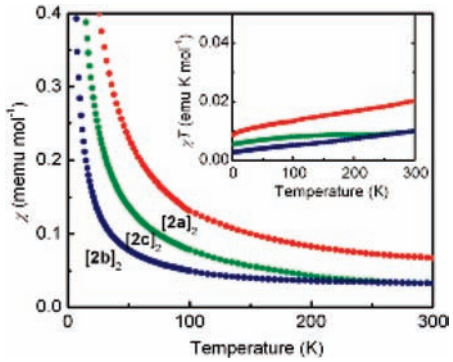

Figure 5. Plots of χ and χT versus temperature for $[\mathbf{2a},\mathbf{b},\mathbf{c}]_2$.

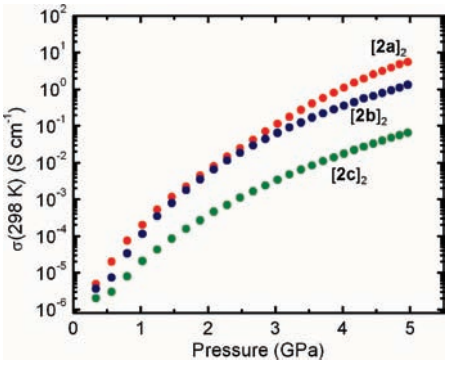

Figure 6. Plots of σ(298 K) versus applied pressure for $[\mathbf{2a},\mathbf{b},\mathbf{c}]_2$.

range 0−5 GPa. That being said, there is a difference in the conductivity of the three compounds at elevated pressures, such that at 5 GPa, σ(298 K) increases from $[\mathbf{2c}]_2$ to $[\mathbf{2b}]_2$ to $[\mathbf{2a}]_2$. This divergence may be related to the greater steric congestion noted above for $[\mathbf{2b}]_2$ and $[\mathbf{2c}]_2$, and as a consequence, a lower compressibility for these compounds.

Discussion

Heterocyclic thiazyl radicals are known to associate in a variety of modes, the most common (but not exclusive) involving the cofacial approach of two radicals to form weak links between one or more sulfurs; examples include 1,2,4,6-thiatriazinyls **6**,[33] 1,2,3,5-dithiadiazolyls **7**,[18,34] 1,3,2-dithiazolyls **8**,[35] and 1,2,3-dithiazolyls **9**[36] (Chart 3). The corresponding selenium-based radicals generally follow suit, although some more unusual modes of association have also been observed.[19,33b] In the pyridine-bridged bisdithiazolyls **1**, spin delocalization is greater, and the potential energetic gain associated with interannular S−S bond formation is less. That being said, there is one example of a pyrazine-bridged bisdithiazolyl **10** that does associate in the solid state.[37] The kinetically favored dimer α-$[\mathbf{10}]_2$ consists of a butterfly like structure in which C−C σ-bond formation successfully competes with spin delocalization. Sublimation and dissociation of this material affords a second, thermodynamically favored polymorph β-$[\mathbf{10}]_2$, in which two radicals are linked laterally by a hypervalent disulfide linkage akin to the Se−Se bond in $[\mathbf{2a},\mathbf{b},\mathbf{c}]_2$.

Outside of thiazyl and selenazyl chemistry, radicals which dimerize via hypervalent disulfide/diselenide linkages are rare, although the tetrathiophenalenyl radical **11** has been

Chart 3

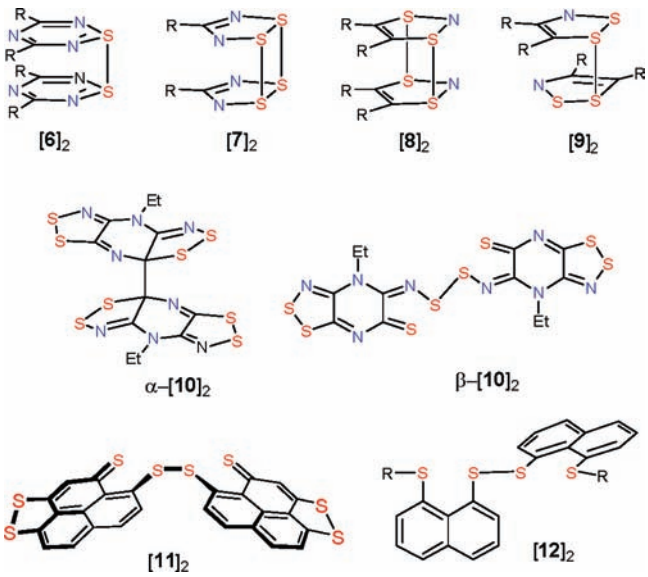

recently shown to associate in this manner.[38] However, in contrast to β-$[\mathbf{10}]_2$ and $[\mathbf{2a},\mathbf{b},\mathbf{c}]_2$ the torsion angle about the disulfide unit (138.2°) is such that the dimer $[\mathbf{11}]_2$ is far from planar, a situation reminiscent of that seen in the disulfide $[\mathbf{12}]_2$,[39] where the lone pair stabilizing the hypervalent center is on a saturated sulfur. Hypervalent dichalcogenides RE-ER (E = S, Se, Te) of this latter type, in which the dichalcogen bond is coordinated on either side by lone pairs on saturated centers,[40] are relatively common, but homonuclear dissociation of such species into radicals has not been observed, presumably because spin density on the resulting radical would be largely localized on the chalcogen, rather than being delocalized onto a heterocyclic ring, as is the case in the present radicals.

Density Functional Theory (B3LYP/6-31G(d,p)) calculations (Table 3) of the bond dissociation enthalpies ΔH_{diss} of the four dimers $[\mathbf{1}]_2$ to $[\mathbf{4}]_2$ (with $R_1 = R_2 = H$) have indicated that σ-dimerization is most favorable for radicals of type **2**, which have selenium located in the 2-position and sulfur in the 1-position. This can be rationalized in terms of the fact

(33) (a) Hayes, P. J.; Oakley, R. T.; Cordes, A. W.; Pennington, W. T. *J. Am. Chem. Soc.* **1985**, *107*, 1346. (b) Bestari, K.; Cordes, A. W.; Oakley, R. T.; Young, K. M. *J. Am. Chem. Soc.* **1990**, *112*, 2249.

(34) (a) Vegas, A.; Pérez-Salazar, A.; Banister, A. J.; Hey, R. G. *J. Chem. Soc., Dalton Trans.* **1980**, 1812. (b) Banister, A. J.; Rawson, J. M. *Adv. Heterocycl. Chem.* **1995**, *62*, 137.

(35) (a) Awere, E. G.; Burford, N; Haddon, R. C.; Parsons, S.; Passmore, J.; Waszczak, J. V.; White, P. S. *Inorg. Chem.* **1990**, *29*, 4821. (b) Awere, E. G.; Burford, N.; Mailer, C.; Passmore, J.; Schriver, M. J.; White, P. S.; Banister, A. J.; Oberhammer, M.; Sutcliffe, L. H. *J. Chem. Soc., Chem. Commun.* **1987**, 66. (c) Brusso, J. L.; Clements, O. P.; Haddon, R. C.; Itkis, M. E.; Leitch, A. A.; Oakley, R. T.; Reed, R. W.; Richardson, J. F. *J. Am. Chem. Soc.* **2004**, *126*, 14692. (d) Alberola, A.; Clements, O. P.; Collis, R. J.; Cubbitt, L.; Grant, C. M.; Less, R. J.; Oakley, R. T.; Rawson, J. M.; Reed, R. W.; Robertson, C. M. *Cryst. Growth Des.* **2008**, *8*, 155.

(36) Barclay, T. M.; Beer, L.; Cordes, A. W.; Oakley, R. T.; Preuss, K. E.; Taylor, N. J.; Reed, R. W. *Chem. Commun.* **1999**, 531.

(37) Leitch, A. A.; McKenzie, C. E.; Oakley, R. T.; Reed, R. W.; Richardson, J. F.; Sawyer, L. D. *Chem. Commun.* **2006**, 1088.

(38) Beer, L.; Reed, R. W.; Robertson, C. M.; Oakley, R. T.; Tham, F. S.; Haddon, R. C. *Org. Lett.* **2008**, *10*, 3121.

(39) Nakanishi, W.; Hayashi, S.; Arai, T. *Chem. Commun.* **2002**, 2416.

(40) (a) Sharma, S.; Selvakumar, K.; Singh, V. P.; Zade, S. S.; Singh, H. B. *Phosphorus, Sulfur Silicon Relat. Elem.* **2008**, *183*, 827. (b) Kandasamy, K.; Kumar, S.; Singh, H. B.; Wolmershäuser, G. *Organometallics* **2003**, *22*, 5069.

Table 3. B3LYP/6-31G(d,p) Dimer Dissociation Enthalpies

Dimer[a]	$[\mathbf{1}]_2$	$[\mathbf{2}]_2$	$[\mathbf{3}]_2$	$[\mathbf{4}]_2$
ΔH_{diss}[b]	11.12	18.19	−1.123	8.87

[a] With $R_1 = R_2 = H$. [b] In kcal mol^{-1}.

that the lighter chalcogen (sulfur) can form a strong π-bond to carbon, while the heavier chalcogen (selenium) is better able to form a hypervalent intermolecular σ-bond. In light of these results it would not be unreasonable to assume that σ-dimerization would be the rule rather than the exception for radicals of type **2**. However, as the structural summary shown in Table 4 illustrates, the size of the R_1/R_2 ligands has a profound influence on the solid state packing of the radicals, and hence their tendency to dimerize. When small R_1/R_2 groups (Me, H, F) are present, packing of the radicals is not compromised by steric constraints, and instead is driven by structure-making four-center Se---N′ interactions, the so-called secondary bonding interactions which are known to be of importance in determining the supramolecular chemistry of heavy chalcogens.[32] Accordingly crystallization of **2a**,**b**,**c** occurs in the (relatively) low symmetry monoclinic space group $P2_1/c$, which allows for the generation of ribbons of radicals bridged by four-center Se---N′ interactions that span centers of inversion. Once linked in this manner, adjacent rings are held in an approximately coplanar arrangement, as illustrated in Scheme 2, and this allows a relatively facile least-motion conversion of intramolecular S−Se bonds into intermolecular Se---Se′ bonds, to produce the closed-shell dimers $[\mathbf{2a},\mathbf{b},\mathbf{c}]_2$. By contrast, larger R_1/R_2 groups lead to clustering of the radicals into higher symmetry packing motifs that preclude the development of four-center Se---N′ interactions. For example, when $R_1 = Et$ and $R_2 = Br$, Cl, Me, **2** crystallizes in the tetragonal space group $P\bar{4}2_1m$, in which four *undimerized* radicals are related by a $\bar{4}$ point.[16] In the case of $R_1 = Me$, $R_2 = Cl$, the space group is $P2_1/n$, but the clustering of the radicals about the inversion centers is such that there are no four-center Se---N′ contacts, indeed the packing of the π-stacks is reminiscent of that seen in the tetragonal structures.[13] Finally, when $R_1 = Me$, Et, and $R_2 =$ Ph, the trigonal space group $P3_121$(or $P3_221$) is found, in which *undimerized* radicals adopt a helical packing arrangement about a 3-fold screw axis.[12a,c] It therefore appears that the size of the R_1 and R_2 groups plays a critical role in determining the structural (spin state) outcome.

Summary and Conclusion

Bisthiaselenazolyl radicals **2** are calculated to be thermodynamically unstable with respect to their σ-bonded dimers $[\mathbf{2}]_2$. Whether or not σ-dimerization actually occurs in the solid state depends on the size of the exocyclic ligands R_1 and R_2, and the influence they have on crystal packing. Large substituents militate against the thermodynamic tendency to dimerize, but when R_1 and R_2 are small, as in the radicals **2a**, **b**,**c** described here, dimerization is observed. The three dimers $[\mathbf{2a},\mathbf{b},\mathbf{c}]_2$ adopt the same crystal structure, which consists of interpenetrating, cross-braced π-stacks. The resulting diamagnetic materials are small band gap semiconductors, with room temperature conductivity values near 10^{-6} S cm^{-1}. Like the initially reported compound $[\mathbf{2a}]_2$, dimers $[\mathbf{2b},\mathbf{c}]_2$ both show a remarkable pressure dependence, increasing by five (for R_2 = Me) to six (for R_2 = F) orders of magnitude under an applied pressure of only 5 GPa. The origin of the effect remains, however, unclear. Whether it involves the closure of a band gap, or a molecular rearrangement, has yet to be determined. High pressure structural studies on these systems are currently under investigation.

Table 4. Space Groups and Association Preferences for Derivatives of **2**

R_1	R_2	space group	spin state	reference
Me	H	$P2_1/c$	σ-dimer	17
Me	F	$P2_1/c$	σ-dimer	this work
Me	Me	$P2_1/c$	σ-dimer	this work
Et	H	$P2_1/c$	σ-dimer	17
Me	Cl	$P2_1/n$	radical	13
Me	C_6H_5	$P3_121$	radical	12a, 12c
Et	C_6H_5	$P3_221$	radical	12a, 12c
Et	Me	$P\bar{4}2_1m$	radical	16
Et	Cl	$P\bar{4}2_1m$	radical	16
Et	Br	$P\bar{4}2_1m$	radical	16

Experimental Section

General Procedures and Starting Materials. The reagents 2,4,6-trifluoropyridine, sulfur monochloride, selenium dioxide, methyl trifluoromethanesulfonate (triflate), ammonia and octamethylferrocene (OMFc) were obtained commercially. Compounds [**1a**][OTf][10b] and [**1c**][OTf][10c] were prepared according to literature methods. OMFc was purified by sublimation in vacuo and recrystallization from acetonitrile. The solvents acetonitrile (MeCN), dichloroethane (DCE), acetic acid (HOAc), diethyl ether (Et_2O), and dichloromethane (DCM) were of at least reagent grade. MeCN was dried by distillation from P_2O_5 and/or CaH_2, and DCE by distillation from P_2O_5. All reactions were performed under an atmosphere of dry nitrogen. Melting points are uncorrected. Infrared spectra (Nujol mulls, KBr optics) were recorded on a Nicolet Avatar FTIR spectrometer at 2 cm^{-1} resolution. ^{1}H spectra were run on a Bruker Avance 300 MHz NMR spectrometer, and low resolution ESI mass spectra were run on a Micromass Q-TOF Ultima Global LC/MS/MS system. Elemental analyses were performed by MHW Laboratories, Phoenix, AZ 85018.

Preparation of *N*-methyl-2,4,6-trifluoropyridinium Triflate. Methyl triflate (1.80 g, 11.0 mmol) and 2,4,6-trifluoropyridine (1.33 g, 10.0 mmol) were charged into a Schlenk tube, and the mixture was stirred and heated in an oil bath at 60 °C. After a few minutes crystals were present, and after 2 h the mixture was completely solid. The mixture was cooled, and 5 mL DCE was added to break up the solid, which was filtered off and washed with 20 mL Et_2O. The crude product, *N*-methyl-2,4,6-trifluoropyridinium triflate, yield 2.70 g (9.1 mmol, 91%), was used without purification, but for analytical purposes it could be recrystallized from MeCN/DCE, mp 114−117 °C. IR: 3060(m), 1682 (s), 1646 (m), 1604 (s), 1539 (m), 1505 (m), 1265 (s, br), 1226 (m), 1149 (s), 1028 (s), 1012 (m), 889 (s), 874 (s), 758 (m), 713 (m), 638 (s), 574 (m), 517 (s), 459 (m) cm^{-1}. ^{1}H NMR (CD_3CN): 7.64 (*dd*, 2H, aromatic, $J_F = 6.98$, 2.13 Hz), 4.01 (*t*, 3H, methyl, $J_F =$ 2.78 Hz). Anal. Calcd for $C_7H_5F_6NO_3S$: C, 28.29; H, 1.70; N, 4.71%. Found: C, 28.28; H, 1.75; N, 4.75%.

Preparation of *N*-methyl-2,6-diamino-4-fluoropyridinium Triflate [5b][OTf]. Anhydrous ammonia was passed over a stirred solution of *N*-methyl-2,4,6-trifluoropyridinium triflate (4.49 g, 15.1 mmol) in 50 mL of dry MeCN held at 0 °C in an ice bath. After 10 min, the ammonia flow was ceased, and the ice bath removed. The solution warmed (heat of reaction) to about 40 °C, turned very slightly yellow, and a gelatinous white precipitate of NH_4F formed. After 30 min the mixture was boiled briefly to expel excess ammonia, then cooled to room temperature, and the white precipitate was filtered off. Evaporation of the solvent from the filtrate afforded a sticky solid that was recrystallized from MeCN/DCE (1:10) to give white flakes of [**5b**][OTf] which were collected by filtration. Yield 3.47 g (11.9 mmol, 79%), mp 126−130 °C. IR: 3428 (m),

Scheme 2

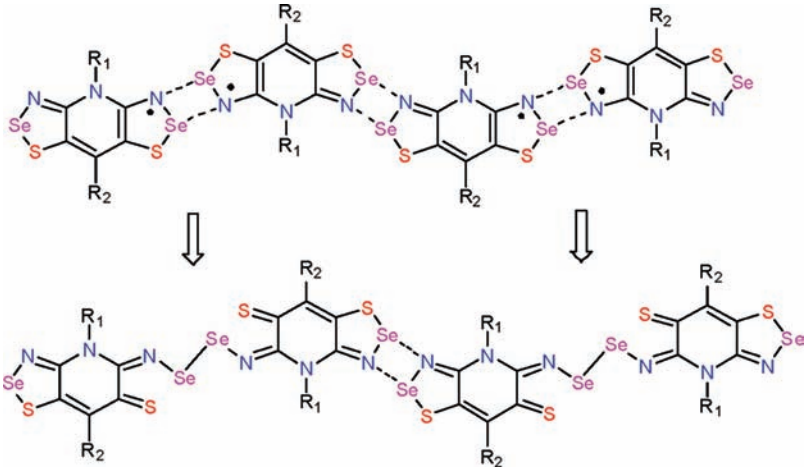

3359 (m), 3242 (m), 1686 (m), 1649 (m), 1593 (m), 1518 (w), 1331 (w), 1277 (s), 1225 (s), 1162 (s), 1027 (s), 809 (m), 706 (m), 722 (m), 634 (s), 575 (w), 518 (m), 456 (m) cm^{-1}. ^1H NMR (CD_3CN): 6.35 (*s*, 2H, amine), 6.00 (*d*, 1H, aromatic, $J_F = 9.56$ Hz), 3.40 (*s*, 3H, methyl). Anal. Calcd for $C_7H_9F_4N_3O_3S$: C, 28.87; H, 3.11; N, 14.43%. Found: C, 28.69; H, 3.22; N, 14.17%.

Preparation of 8-Fluoro-4-methyl-4*H*-bis[1,2,3]dithiazolo[4,5-b:5′,4′-e]pyridin-2-ium Triflate [1b][OTf]. A solution of S_2Cl_2 (2.16 g, 16.0 mmol) in 5 mL MeCN was added dropwise to a solution of [**5b**][OTf] (1.16 mg, 4.00 mmol) in 10 mL of MeCN, and the mixture heated to a gentle reflux under an atmosphere of nitrogen. After 1.5 h the mixture was cooled to room temperature, and the light brown microcrystalline precipitate of crude [**1b**][OTf] (0.68 g, 1.65 mmol, 41%) was filtered off, washed with 3 × 20 mL hot DCE, and dried in vacuo. Recrystallization from MeCN afforded deep red plates, dec > 295 °C. IR: 1510 (s), 1352 (m), 1280 (m), 1238 (s), 1174 (m), 1161 (w), 1125 (m), 1059 (w), 1027 (s), 937 (w), 868 (m), 791 (s), 713 (m), 678 (s), 654 (w), 638 (m), 557 (w), 559 (w),516 (m), 500 (w), 479 (s), 472 (s) cm^{-1}. Anal. Calcd for $C_7H_3F_4N_3O_3S_5$: C, 20.34; H, 0.73; N, 10.16%. Found: C, 20.60; H, 0.85; N, 10.11%.

Preparation of 4-Methyl-4*H*-bis[1,2,3]thiaselenazolo[4,5-b:5′,4′-e]pyridin-2-ium Triflate [2a][OTf]. Finely ground selenium dioxide (0.450 g, 4.06 mmol) was added to a solution of [**1a**][OTf] (0.398 g, 1.01 mmol) dissolved in 100 mL of HOAc, and the reaction mixture was set to reflux for 4 h, at which time the heat was removed and the solution allowed to cool slowly. After 16 h, the resulting red crystalline solid was filtered and washed with DCM, crude yield; 0.434 g (0.887 mmol, 89%). The crude material was recrystallized twice from HOAc to afford [**2a**][OTf] as red flakes. The product was identified by comparison to the IR spectrum of a known sample.[17]

Preparation of 8-Fluoro-4-methyl-4*H*-bis[1,2,3]thiaselenazolo[4,5-b:5′,4′-e]pyridin-2-ium Triflate [2b][OTf]. Compound [**1b**][OTf] (0.830 g, 2.01 mmol) and finely ground selenium dioxide (0.670 g, 6.04 mmol) were combined in a large glass pressure vessel along with 80 mL MeCN, and the mixture was stirred in an oil bath at 110 °C for 72 h. After cooling slightly, the warm slurry was filtered through a glass Büchner funnel to remove a small amount of black powder, and the filtrate was concentrated to 30 mL and allowed to stand for 16 h. The resulting red solid was collected by filtration and rinsed with DCM, crude yield; 0.542 g (1.07 mmol, 54%). The crude material was recrystallized from MeCN to afford red needles, dec > 265 °C. IR: 1501 (s), 1350 (m), 1283 (s), 1225 (s), 1175 (m), 1113 (m), 1050 (w), 1004 (s), 854 (w), 773 (s), 716 (m), 637 (s), 596 (s), 515 (m), 494 (w), 477 (w) cm^{-1}. Anal. Calcd for $C_7H_3F_4N_3O_3S_3Se_2$: C, 16.58; H, 0.60; N, 8.28%. Found: C, 16.76; H, 0.57; N, 8.31%.

Preparation of 8-Methyl-4-methyl-4*H*-bis[1,2,3]thiaselenazolo[4,5-b:5′,4′-e]pyridin-2-ium Triflate [2c][OTf]. Finely ground selenium dioxide (0.670 g, 6.04 mmol) was added to a solution of [**1c**][OTf] (0.820 g, 2.00 mmol) dissolved in 140 mL of HOAc, and the reaction mixture was set to reflux for 7 h. At this time the heat was removed, and the solution slowly cooled. After 16 h, the golden brown powder was filtered and rinsed with DCM, crude yield: 0.842 g (1.67 mmol, 84%). Recrystallization from MeCN provided golden flakes, dec > 260 °C. IR: 1407 (m), 1359 (s), 1267 (s), 1239 (s), 1164 (s), 1030 (s), 1009 (m), 777 (w), 723 (s), 641 (s), 594 (s), 540 (m), 517 (m), 481 (m) cm^{-1}. Anal. Calcd for $C_8H_6F_3N_3O_3S_3Se_2$: C, 19.09; H, 1.20; N, 8.35%. Found: C, 18.99; H, 1.11; N, 8.26%.

Preparation of Dimers [2a,b,c]$_2$. Degassed solutions (3 freeze−pump−thaw cycles) of [**2a,b,c**][OTf] (0.596−0.690 mmol) in 210−225 mL of MeCN and OMFc (0.657−0.758 mmol) in 108−125 mL of MeCN were combined, and after 30 min the gold-brown microcrystalline precipitate of [**2a,b,c**]$_2$ was filtered off, washed with 5×30 mL MeCN, and dried in vacuo. Analytical data: [**2a**]$_2$. Identified by comparison with the IR spectrum of a known sample, previously reported.[17] [**2b**]$_2$. IR: 1522 (s), 1488 (m), 1438 (s), 1360 (m), 1304 (s), 1200 (w), 1176 (m), 1093 (m), 1036 (m), 853 (s), 765 (s), 712 (w), 610 (s), 564 (s) cm^{-1}. Anal. Calcd for $C_6H_3FN_3S_2Se_2$: C, 20.12; H, 0.84; N, 11.73%. Found: C, 20.37; H, 0.93; N, 11.81%. [**2c**]$_2$. IR: 1505 (s), 1382 (m), 1342 (s), 1306 (s), 1174 (w), 1062 (w), 1008 (s), 842 (m), 715 (s), 608 (m), 568 (s), 522 (m), 464 (w) cm^{-1}. Anal. Calcd for $C_7H_6N_3S_2Se_2$: C, 23.74; H, 1.71; N, 11.86%. Found: C, 24.00; H, 1.90; N, 11.83%.

Powder X-ray Diffraction. Powdered samples (ca. 60 mg) of [**2b**,**c**]$_2$ were loaded into an aluminum sample holder which was rotated during data collection. The X-ray diffraction data was collected on a powder diffractometer with a position sensitive detector (INEL) at ambient temperature using Cu Kα_1 radiation ($\lambda = 1.5406$ Å). The total 2θ range was 0−112°, measured in steps of 0.029°. The powder diffraction patterns were indexed by the program TAUP,[41] from which it was evident that both compounds were isostructural with [**2a**]$_2$ and the space group $P2_1/c$ was selected. Starting with the molecular coordinates for [**2a**]$_2$ as the initial model, with the F atom (in [**2b**]$_2$) and Me group (in [**2c**]$_2$) introduced in calculated positions, the structures were solved using FOX[42] and/or DASH,[43] and the unit cell dimensions were refined by Rietveld methods[44] using the GSAS

(41) Taupin, D. G. *J. Appl. Crystallogr.* **1969**, *2*, 179.
(42) Favre-Nicolin, V.; Cerny, R. *J. Appl. Crystallogr.* **2002**, *35*, 734.
(43) David, W. I. F.; Shankland, K.; van de Streek, J.; Pidcock, E.; Motherwell, W. D. S.; Cole, J. C. *J. Appl. Crystallogr.* **2006**, *39*, 910.
(44) Rietveld, H. M. *J. Appl. Crystallogr.* **1969**, *2*, 65.
(45) Larson, A. C.; Von Dreele, R. B. Report No. LA-UR-86-748; Los Alamos National Laboratory: Los Alamos, NM, 1987.

program package.[45] Atomic positions obtained from DASH and/or FOX were not further refined in GSAS; as a result standard deviations for atomic coordinates are not available. Final Rietveld indices R_p and R_{wp} are listed in Table 1.

Magnetic Susceptibility Measurements. Direct current (DC) magnetic susceptibility measurements on $[\mathbf{2a},\mathbf{b},\mathbf{c}]_2$ were performed over the range 2−300 K on a Quantum Design MPMS SQUID magnetometer operating at $H = 1000$ Oe. Diamagnetic corrections were made using Pascal's constants.[46]

High Pressure Conductivity Measurements. High pressure temperature conductivity experiments on $[\mathbf{2a},\mathbf{b},\mathbf{c}]_2$ were carried out in a cubic anvil press[47] using pyrophyllite ($Al_4Si_8O_{20}(OH)_4$) as the pressure transmitting medium. Sample pressure was determined from previous calibrations of the applied hydraulic load against pressures of structure transformations in standards at room temperature (Hg L ↔ I at 0.75 GPa, Bi I ↔ II at 2.46 GPa, Tl 1 ↔ III at 3.70 GPa, and Ba 1 ↔ II at 5.5 GPa).[48] Two Pt electrodes contacted the pre-compacted, powder samples which were contained in a boron nitride ($\sigma_{BN} \approx 10^{-11}$ S cm^{-1}) cup. Four-wire ac (Solartron 1260 Impedance Analyzer) resistance measurements were made at a frequency of 1 kHz. The contiguous disk-shaped sample was extracted from the recovered pressure cell, and the sample geometry was measured to convert resistance to conductivity.

Electronic Structure Calculations. The association energies of radicals **1**−**4** ($R_1 = R_2 = H$) were estimated using the Gaussian 98W suite of programs[49] in terms of the difference between the total electronic energy (B3LYP/6-31G(d,p)) of the radicals and their respective dimers. Dimer geometries were optimized within a C_{2h} symmetry constraint and were confirmed to be stationary points by frequency calculations.

Acknowledgment. We thank the Natural Sciences and Engineering Research Council of Canada (NSERCC) for financial support. We also acknowledge the NSERCC for a Canada Graduate Scholarship to A.A.L., the Ontario Provincial Government for a Graduate Scholarship to C.M.R., and the Canada Council for a Killam Research Fellowship to R.T.O.

Supporting Information Available: Details of X-ray crystallographic data collection and structure refinement, tables of atomic coordinates, bond distances and angles, anisotropic thermal parameters, and hydrogen atom positions in CIF format. This material is available free of charge via the Internet at http://pubs.acs.org.

(46) Carlin, R. L. *Magnetochemistry*; Springer-Verlag: New York, 1986.
(47) Secco, R. A. *Can. J. Phys.* **1995**, *73*, 287.
(48) Secco, R. A.; Schloessin, H. H. *J. Appl. Phys.* **1986**, *60*, 1625.
(49) Frisch, M. J.; Trucks, G. W.; Schlegel, H. B.; Scuseria, G. E.; Robb, M. A.; Cheeseman, J. R.; Zakrzewski, V. G.; Montgomery, J. A., Jr.; Stratmann, R. E.; Burant, J. C.; Dapprich, S.; Millam, J. M.; Daniels, A. D.; Kudin, K. N.; Strain, M. C.; Farkas, O.; Tomasi, J.; Barons, V.; Cossi, M.; Cammi, R.; Mennucci, B.; Pomelli, C.; Adamo, C.; Clifford, S.; Ochterski, J.; Petersson, G. A.; Ayala, P. Y.; Cui, Q.; Morokuma, K.; Malick, D. K.; Rabuck, A. D.; Raghavachari, K.; Foreman, J. B.; Cioslowski, J.; Ortiz, J. V.; Stefanov, B. B.; Liu, G.; Fox, D. J.; Keith, T.; Al-Laham, M. A.; Peng, C. Y.; Nanayakkara, A.; Wong, M. W.; Andres, J. L.; Gonzalez, C.; Head-Gordon, M.; Repogle, E. S.; Pople, J. A. *Gaussian 98*, Revision A:6; Gaussian, Inc.: Pittsburgh, PA, 1998.